

Structural, Thermodynamic and Magneto-Electronic Properties of $\text{Cd}_{0.75}\text{Cr}_{0.25}\text{Se}$ and $\text{Zn}_{0.75}\text{Cr}_{0.25}\text{S}$: An *Ab-Initio* Study

S. AMARI^{a,b}, S. DAUD^{c,*} AND H. REKAB-DJABRI^{d,e}

^aLaboratoire de Modélisation et Simulation en Sciences des Matériaux, Université Djillali Liabès de Sidi Bel-Abbès, Sidi Bel-Abbès, 22000, Algeria

^bFaculty of Nature and Life Science, Hassiba Benbouali University of Chlef, 02000, Algeria

^cLaboratory of Materials and Electronic Systems, Mohamed El Bachir El Ibrahimi University of Bordj Bou Arreridj, 34000, Bordj Bou Arreridj, Algeria

^dLaboratory of Micro and Nanophysics (LaMiN), National Polytechnic School Oran, ENPO-MA, BP 1523, El M'Naouer, 31000, Oran, Algeria

^eFaculty of Nature and Life Sciences and Earth Sciences, Akli Mohand-Oulhadj University, 10000, Bouira, Algeria

Received: 05.09.2022 & Accepted: 13.12.2022

Doi: [10.12693/APhysPolA.143.36](https://doi.org/10.12693/APhysPolA.143.36)

*e-mail: salah_daoud07@yahoo.fr

Using the full-potential linearized augmented plane wave plus local orbital method based on spin-polarized density functional theory, we investigate the parameters of the structure, the electronic, magnetic, and thermodynamic properties of cubic zinc-blende $\text{Cd}_{0.75}\text{Cr}_{0.25}\text{Se}$ and $\text{Zn}_{0.75}\text{Cr}_{0.25}\text{S}$ ordered ferromagnetic materials. We adopt the Perdew–Burke–Ernzerhof generalized gradient approximation and the modified Becke–Johnson exchange potential for the exchange-correlation energy and potential. Furthermore, the effect of high pressure on the normalized unit cell volume, bulk modulus, and Grüneisen parameter for both CdSe and ZnS binary compounds as well as for $\text{Cd}_{0.75}\text{Cr}_{0.25}\text{Se}$ and $\text{Zn}_{0.75}\text{Cr}_{0.25}\text{S}$ partially substituted materials was also predicted. The results indicate that both these materials are stabilized in the ferromagnetic phase. Using the modified Becke–Johnson approach and Perdew–Burke–Ernzerhof generalized gradient approximation, our calculations also demonstrate that both $\text{Cd}_{0.75}\text{Cr}_{0.25}\text{Se}$ and $\text{Zn}_{0.75}\text{Cr}_{0.25}\text{S}$ alloys are semiconductors with the magnetic moment of $4 \mu_B$ per formula unit. Furthermore, the calculations of the s – d exchange constant and p – d exchange constant clearly indicate the magnetic nature of these compounds. Finally, in order to gain further information, basic thermodynamic properties such as heat capacity, thermal expansion coefficient, and entropy have been explored using the quasi-harmonic Debye model.

topics: density functional theory (DFT), magnetic semiconductors, thermodynamic properties, electronic structure

1. Introduction

Diluted magnetic semiconductors (DMSs) are materials containing small amounts of magnetic impurities. Recently, this family of semiconducting materials has attracted intensive interest [1–3]. An intriguing, and potentially technologically useful, property that arises from applying these materials is the possibility of strongly spin-polarized currents [4]. It is this idea of spin-polarized currents that would allow engineering devices that combine the properties of magnetism with the traditional semiconductors to create the so-called spintronic (also called spin-based electronics or magneto-electronics) devices, which are recently considered a new field in nano-electronics technology.

The electronic structures of the DMSs materials depend firstly on the crystallographic structure of the based crystals and secondly on the doped magnetic impurity atoms. In the case of $\text{Cd}_{0.75}\text{Cr}_{0.25}\text{Se}$ and $\text{Zn}_{0.75}\text{Cr}_{0.25}\text{S}$ partially substituted semiconductors, the bonding interactions in their crystal structures occur between the semiconductor s – p orbitals and the magnetic ions d orbitals. All the physical properties observed in our calculations are the result of this bonding nature.

It has been suggested [5] that one of the variables determining the strength of the exchange interactions is the amount of sp – d hybridization between the host and impurity. From a theoretical point of view, there is an enormous amount of research in the area of $3d$ -doped semiconductors.

For example, Saeed et al. [6] investigated the magnetic and electronic properties, as well as the parameters of the structure of $\text{Cd}_{0.75}\text{Co}_{0.25}\text{X}$ ($\text{X} = \text{S}, \text{Se}, \text{and Te}$) ternary alloys using the full-potential linearized augmented plane wave plus local orbital (FP-L/APW+lo) method. They found that the tetrahedral crystal field gives rise to triple degeneracy t_{2g} and double degeneracy e_g . It was demonstrated by Nazir et al. [7] that the half-metallicity is robust with respect to lattice contraction and is maintained up to compression of the lattice constants by 8% and 6%, respectively.

In the year 2012, Amari et al. [8] found that $\text{Zn}_{0.75}\text{TM}_{0.25}\text{Se}$ ($\text{TM} = \text{Cr}, \text{Fe}, \text{Co}, \text{and Ni}$) ternary alloys are stable in the FM phase, and the cohesive energies of $\text{Zn}_{0.75}\text{TM}_{0.25}\text{Se}$ are greater than that of cubic zinc-blende (B3) ZnSe compound. In the same year, Bourouis and Meddour [9] studied several physical properties of ordered dilute ferromagnetic ternary $\text{Cd}_{1-x}\text{Fe}_x\text{S}$ alloys with $x = 0.25, 0.5, \text{and } 0.75$ in the B3 phase. They have observed that the p - d hybridization of Fe d and S p states reduces the magnetic moment of Fe from its free space charge value and produces the local magnetic moment on the nonmagnetic Cd and S sites. On the other hand, the ferromagnetic behaviors have been confirmed experimentally for several Cr-(DMSs) materials, such as ZnCrSe alloy [10], ZnCrS material [11], ZnCrTe semiconductor [12], and Cd-CrS ternary alloy [13].

However, till now, there are only a few reports on the properties of Cr-doped zinc-blende CdSe and ZnS, either experimental or theoretical. For these reasons, in this work, we have made an attempt to investigate the electronic, magnetic, and thermodynamic properties of Cr-doped zinc-blende CdSe and ZnS through the FP-L/APW+lo method and the quasi-harmonic Debye model approach. Our results are compared to other theoretical and experimental studies. Furthermore, we add some interesting information about these properties. To the author's knowledge, the electronic structure and magnetic properties of Cr-doped CdSe have never been reported in the literature so far. In the following section, we describe the details of our calculations, while in Section 3, we discuss our results. Finally, conclusions will be given in Sect. 4.

2. Computational method

In this paper, all the calculations are performed using the FP-L/APW+lo approach based on the spin-polarized density functional theory (SP-DFT), as implemented in the WIEN2K code [14]. For the exchange-correlation functional, the generalized gradient approximation of Perdew–Burke–Ernzerhof (GGA-PBE) [15] and the modified Becke–Johnson approach (mBJ) [16] are used. On the basis of convergence tests on our response functions with a varying number of k points, we are confident that 150 k points and basis functions up

to $R_{MT}K_{\text{max}} = 8.00$ ensure an accurate and well-converged result. The doped composition is optimized totally with respect to both the atomic positions and the lattice constants. Self-consistency is achieved when the total energy difference between the successive iterations is less than 10^{-4} Ry per supercell. CdSe and ZnS binary compounds have a B3 structure with space group $F-43m$, whose experimental lattice constants are 6.05 Å [17] and 5.41 Å [17], respectively. The structure of $\text{Cd}_{1-x}\text{Cr}_x\text{Se}$ and $\text{Zn}_{1-x}\text{Cr}_x\text{S}$ at $x = 0.25$ are obtained by replacing the Cd/Zn atoms at the (0, 0, 0) position with Cr in the unit cell of the (B3) CdSe or ZnS. The muffin-tin radii were chosen to be 2.4 Bohr for Cd, Zn, and Cr atoms and 2.0 for S and Se atoms, respectively. In the calculation, the $3d^{10}4s^2$ states of Zn, $4d^{10}5s^2$ states of Cd, $3s^23p^4$ states of S, and $3d^54s^1$ states of Cr are treated as valence configurations. The thermodynamic properties are investigated within the framework of the quasi-harmonic Debye model [18]. Detailed descriptions of the thermodynamic properties calculation procedure can be found in [19–22].

3. Results and discussion

3.1. Structural and thermodynamic properties

In order to give more information on the structural properties of bulk $\text{Cd}_{0.75}\text{Cr}_{0.25}\text{Se}$ and $\text{Zn}_{0.75}\text{Cr}_{0.25}\text{S}$ alloys, the total energy E was calculated as a function of the unit cell volume V . The equilibrium parameters, especially the lattice constant a_0 , the bulk modulus B_0 , the pressure derivative of the bulk modulus B'_0 , and the cohesive energy E_{coh} for $\text{Cd}_{0.75}\text{Cr}_{0.25}\text{Se}$ and $\text{Zn}_{0.75}\text{Cr}_{0.25}\text{S}$ have been obtained by fitting the calculated values of the total energy versus volume (E - V) using the Murnaghan equation of state [23]. The numerical values obtained from different quantities are given in Table I. For comparison, some other data from the literature [7, 17, 24, 25] are also presented in Table I. It is very clear that our results for CdS and ZnS compounds nicely agree with the experiments and other theoretical data. For $\text{Zn}_{0.75}\text{Cr}_{0.25}\text{S}$ ternary, the results are in good agreement with the theoretical data [7], while for $\text{Cd}_{0.75}\text{Cr}_{0.25}\text{Se}$, there are no theoretical or experimental data available in the literature yet.

We also calculated ($\Delta E = E_{\text{AFM}} - E_{\text{FM}}$) between anti-ferromagnetic (AFM) and ferromagnetic (FM) states, and it can be seen that the ferromagnetic state is more stable than the anti-ferromagnetic state. The cohesive energies of these compounds are also calculated from the difference between the total atomic energies of Cd, Zn, Cr, S, and Se atoms and the minimum energy of bulk compounds, which are also presented in Table I.

It is observed that the cohesive energies of binary compounds CdSe and ZnS are lower than those of the ternary compounds. As already explained

Calculated structural parameters for CdSe, Cd_{0.75}Cr_{0.25}Se, ZnS, and Zn_{0.75}Cr_{0.25}S materials.

TABLE I

Material	Reference	a_0 [Å]	B_0 [GPa]	B'_0	ΔE [meV]	E_{coh} [eV]
CdSe	This work	6.16	50.20	4.06	–	4.45
	Ref. [17]	6.05	53.00	–	–	–
	Ref. [24]	6.08	56.79	5.00	–	–
Cd _{0.75} Cr _{0.25} Se	This work	6.09	52.27	5.33	77	5.49
ZnS	This work	5.44	73.99	4.43	–	6.34
	Ref. [17]	5.41	74.80	5.40	–	–
	Ref. [25]	5.73	91.57	5.40	–	–
Zn _{0.75} Cr _{0.25} S	This work	5.43	74.50	4.57	61	6.33
	Ref. [7]	5.36	66.16	4.49	65	7.56

in [25, 26], this difference in the value of cohesive energy can be attributed to the lower spin-polarized energy ΔE_{SP} that can occur when a free atom having localized orbitals is transferred to the solid that obviously have less localized orbitals, and to the effect of $3d$ or $4d$ electrons of transition-metal atoms.

Several empirical expressions have usually been used to predict the bulk modulus B of materials from their structural parameters. For example, in I–VII, II–VI, and III–V binary materials having cubic CsCl, NaCl, and ZnS-type structures, the bulk modulus B and the inter-ionic separation r_0 are related by the following exponential relationship $B = Cr_0^{-n}$ [27], where C and n are two constants. For the II–VI group with B3 configuration, the numerical values of C and n are 7.6 and -2.83, respectively [27]. By substituting our values of r_0 into the previous empirical expression, the values of B were found to be 48.87 GPa for Cd_{0.75}Cr_{0.25}Se alloy and 67.61 GPa for Zn_{0.75}Cr_{0.25}S, respectively. These two B values are slightly lower than the results obtained from the fits of the E – V data.

It is well known that the crystal packing of solid and its electronic structure was considerably influenced by applying high pressures [28]. Under high hydrostatic compression, the zinc-blende (B3) structure of CdSe transforms to the rock-salt (B1) phase at the pressure of around 2.87 GPa [29], while for the ZnS compound, the transition pressure from B3 to B1 was reported between the limits of 14.7 and 17.4 GPa, respectively [30]. In order to see how the volume of a unit cell changes with increasing pressure, the values of the normalized volume $V(p)/V_0$ for both Cd_{0.75}Cr_{0.25}Se and Zn_{0.75}Cr_{0.25}S alloys have been calculated from the Vinet equation of state (EOS) [31]. The variations of the relative volume $-\Delta V(p)/V_0 = (V_0 - V(p))/V_0$ as a function of pressure p ranging from 0 to 2.87 GPa for both CdSe and Cd_{0.75}Cr_{0.25}Se, and from 0 to 14.7 GPa for both ZnS and Zn_{0.75}Cr_{0.25}S were illustrated in Fig. 1.

It can be seen that $(V_0 - V(p))/V_0$ for all materials increases with increasing pressure p . As the pressure varies from 0 to 2.87 GPa, $-\Delta V(p)/V_0$ values for Cd_{0.75}Cr_{0.25}Se change from 0 to 0.047, while these

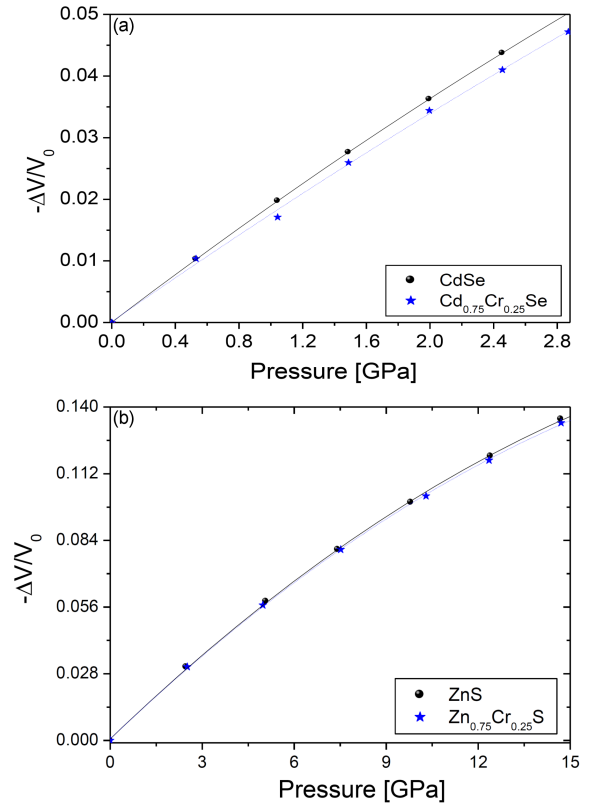


Fig. 1. Relative volume $(V_0 - V(p))/V_0$ vs pressure p for CdSe, Cd_{0.75}Cr_{0.25}Se, ZnS and Zn_{0.75}Cr_{0.25}S.

of Zn_{0.75}Cr_{0.25}S increase from 0 to 0.133, as the pressure varies from 0 to 14.7 GPa, respectively. The variations of the cell dimensions are fitted with the least squares to a linear combination of 2nd order polynomials of pressure p :

$$-\frac{\Delta V}{V_0} = 2.88 \times 10^{-5} + 1.97 \times 10^{-2}p - 7.72 \times 10^{-4}p^2 \quad (\text{for CdSe}), \quad (1)$$

$$-\frac{\Delta V}{V_0} = 1.54 \times 10^{-4} + 1.80 \times 10^{-2}p - 5.40 \times 10^{-4}p^2 \quad (\text{for Cd}_{0.75}\text{Cr}_{0.25}\text{Se}), \quad (2)$$

$$-\frac{\Delta V}{V_0} = 6.77 \times 10^{-4} + 1.24 \times 10^{-2}p - 2.24 \times 10^{-4}p^2 \quad (\text{for ZnS}), \quad (3)$$

$$-\Delta V/V_0 = 7.02 \times 10^{-4} + 1.23 \times 10^{-2}p - 2.24 \times 10^{-4}p^2 \quad (\text{for Zn}_{0.75}\text{Cr}_{0.25}\text{S}), \quad (4)$$

where $-\frac{\Delta V}{V_0}$ is dimensionless, and the pressure p is expressed in GPa.

As illustrated in Fig. 1, it is clear that at high pressures, the relative volume variation $-\frac{\Delta V(p)}{V_0}$ values of $\text{Zn}_{0.75}\text{Cr}_{0.25}\text{S}$ are smaller than those of $\text{Cd}_{0.75}\text{Cr}_{0.25}\text{Se}$ alloy, indicating that later material is more compressible than $\text{Zn}_{0.75}\text{Cr}_{0.25}\text{S}$.

If we assume the model of the equation of state proposed by Vinet [31], the pressure dependence of the isothermal bulk modulus B may be determined as follows [31, 32]:

$$B = B_0 x^{-2} \left[1 + (\eta x + 1)(1 - x) \right] e^{\eta(1-x)}, \quad (5)$$

where $x = (V/V_0)^{1/3}$ and $\eta = 3(B'_0 - 1)/2$.

Figure 2 shows the pressure dependence of the compression module B for CdSe, $\text{Cd}_{0.75}\text{Cr}_{0.25}\text{Se}$, ZnS, and $\text{Zn}_{0.75}\text{Cr}_{0.25}\text{S}$. As shown in Fig. 2, B increases with increasing pressure p for all our materials of interest. Similar qualitative behavior of B vs pressure has been reported for MgCu intermetallic compound [33], MgCa material [34], AlY intermetallic compound [35], hexanitrohexaazaisowurtzitan material (ε -CL-20) [36], silicon carbide (3C-SiC) [37], and Mn_2NiGe heusler compound [38]. As the pressure varies from 0 to 2.87 GPa, the bulk modulus B values for $\text{Cd}_{0.75}\text{Cr}_{0.25}\text{Se}$ increase from 52.27 to 66.95 GPa, while these of $\text{Zn}_{0.75}\text{Cr}_{0.25}\text{S}$ change from 74.5 to 135.11 GPa, as the pressure rises from 0 to 14.7 GPa, respectively.

It is conventional to fit the bulk modulus B versus pressure to linear form [33], but sometimes the 2nd order polynomial form is used $B(p) = B_0 + \alpha p + \beta p^2$ [31, 39]. The best fits of our data on B [GPa] versus pressure p [GPa] obey the following expressions

$$B = 50.20 + 4.05p - 4.54 \times 10^{-2}p^2 \quad (\text{for CdSe}), \quad (6)$$

$$B = 52.27 + 5.31p - 6.84 \times 10^{-2}p^2 \quad (\text{for Cd}_{0.75}\text{Cr}_{0.25}\text{Se}), \quad (7)$$

$$B = 74.04 + 4.34p - 2.37 \times 10^{-2}p^2 \quad (\text{for ZnS}), \quad (8)$$

$$B = 74.56 + 4.47p - 2.45 \times 10^{-2}p^2 \quad (\text{for Zn}_{0.75}\text{Cr}_{0.25}\text{S}). \quad (9)$$

As shown in Fig. 2, the incorporation of 25% Cr atoms into CdSe and ZnS crystals increases the bulk modulus B for $\text{Cd}_{0.75}\text{Cr}_{0.25}\text{Se}$ alloy but not for $\text{Zn}_{0.75}\text{Cr}_{0.25}\text{S}$.

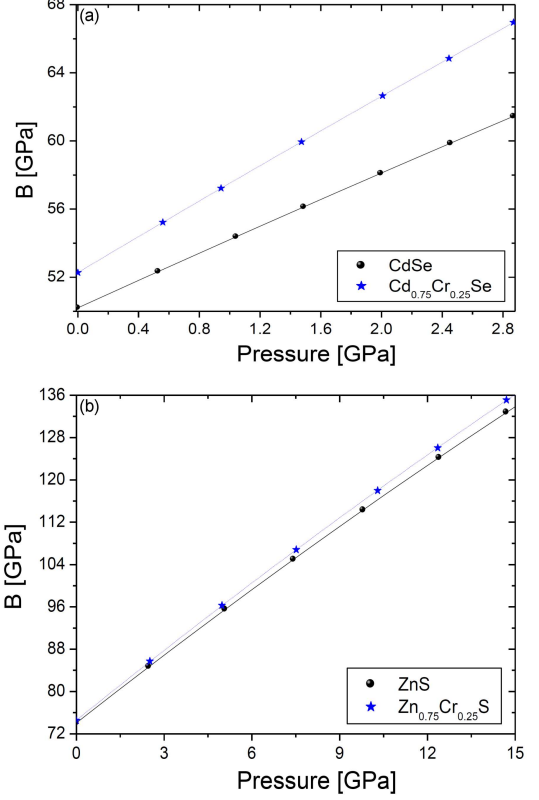


Fig. 2. Bulk modulus B versus pressure p for (a) CdSe, $\text{Cd}_{0.75}\text{Cr}_{0.25}\text{Se}$, and (b) ZnS, $\text{Zn}_{0.75}\text{Cr}_{0.25}\text{S}$ materials.

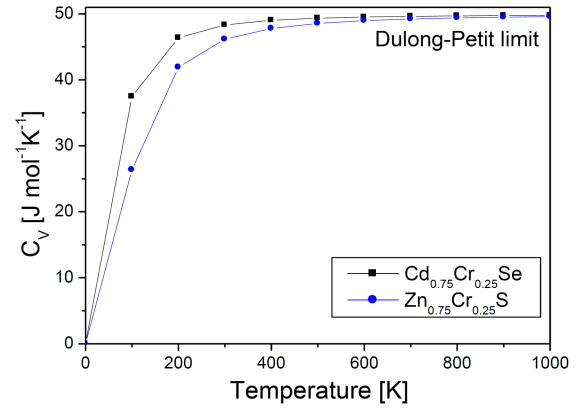


Fig. 3. Temperature dependence of C_V for $\text{Cd}_{0.75}\text{Cr}_{0.25}\text{Se}$ and $\text{Zn}_{0.75}\text{Cr}_{0.25}\text{S}$ materials.

Figure 3 demonstrates the evolution of the heat capacity at constant volume C_V vs temperature T for $\text{Cd}_{0.75}\text{Cr}_{0.25}\text{Se}$ and $\text{Zn}_{0.75}\text{Cr}_{0.25}\text{S}$ alloys. The C_V increases with the increase in temperature and then tends to the Dulong–Petit limit [38, 40].

The heat capacity C_V at high temperature approaches approximately $49.5 \text{ J mol}^{-1} \text{ K}^{-1}$ in both alloys. At room temperature, the obtained C_V values for $\text{Cd}_{0.75}\text{Cr}_{0.25}\text{Se}$ and $\text{Zn}_{0.75}\text{Cr}_{0.25}\text{S}$ alloys are $48.32 \text{ J mol}^{-1} \text{ K}^{-1}$ and $46.15 \text{ J mol}^{-1} \text{ K}^{-1}$,

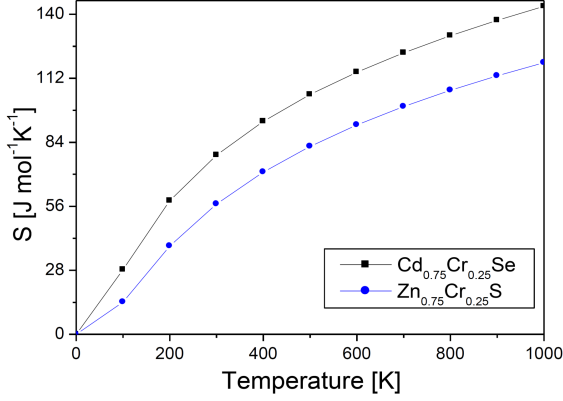


Fig. 4. Temperature dependence of the entropy S for $\text{Cd}_{0.75}\text{Cr}_{0.25}\text{Se}$ and $\text{Zn}_{0.75}\text{Cr}_{0.25}\text{S}$ materials.

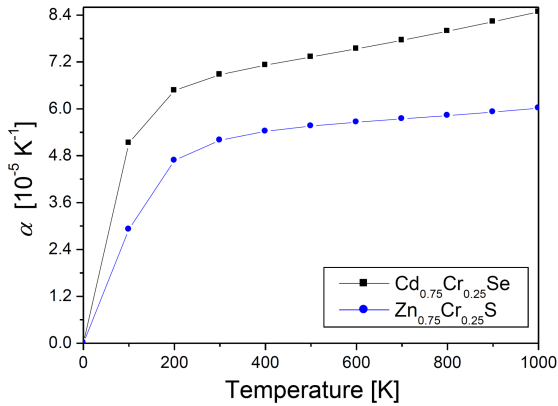


Fig. 5. Thermal expansion coefficient vs temperature for $\text{Cd}_{0.75}\text{Cr}_{0.25}\text{Se}$ and $\text{Zn}_{0.75}\text{Cr}_{0.25}\text{S}$ alloys.

respectively. Our results show that below 300 K, $\text{Cd}_{0.75}\text{Cr}_{0.25}\text{Se}$ has the largest C_V , which can be explained by the fact that Cd has a larger mass compared to Zn.

Next, we figure out the variation of the entropy S with temperature depicted in Fig. 4. It can be seen that the entropy S increases with the increase of temperature T . Similar qualitative behavior of the entropy S versus temperature has been reported for (3C-SiC) material [37], and cubic rock-salt thulium arsenide (TmAs) compound [41]. We note that the entropy S of $\text{Cd}_{0.75}\text{Cr}_{0.25}\text{Se}$ remains higher than that of $\text{Zn}_{0.75}\text{Cr}_{0.25}\text{S}$ at all temperatures. At $T = 300$ K, the entropy S is $78.4 \text{ J mol}^{-1} \text{ K}^{-1}$ for $\text{Cd}_{0.75}\text{Cr}_{0.25}\text{Se}$ and $57 \text{ J mol}^{-1} \text{ K}^{-1}$ for $\text{Zn}_{0.75}\text{Cr}_{0.25}\text{S}$, respectively.

One of the distinct factors is the thermal expansion coefficient (α) which describes the nature of bonding among the constituent atoms. Figure 5 depicts the varying of α with temperature for both $\text{Cd}_{0.75}\text{Cr}_{0.25}\text{Se}$ and $\text{Zn}_{0.75}\text{Cr}_{0.25}\text{S}$ alloys.

It is clear that α increases with T^3 at low temperatures and gradually approaches a linear increase at high temperatures. No available results, neither

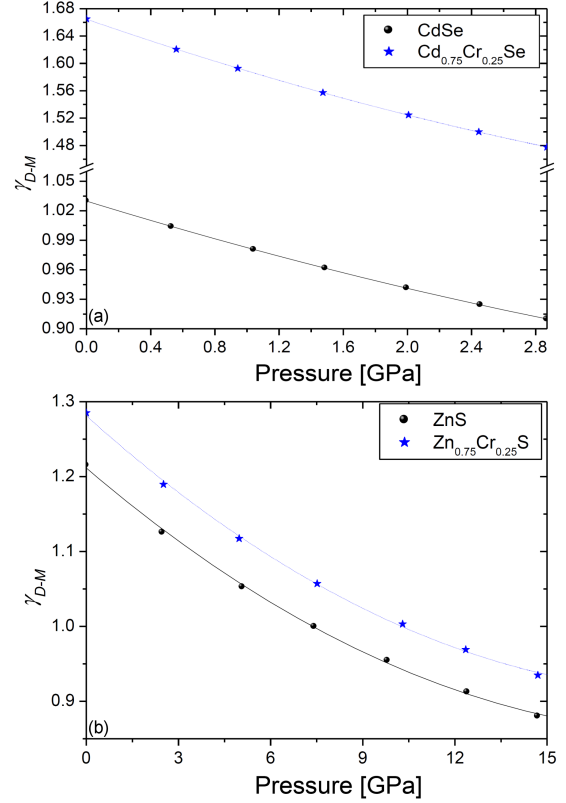


Fig. 6. Grüneisen parameter γ_{D-M} vs pressure p for (a) CdSe , $\text{Cd}_{0.75}\text{Cr}_{0.25}\text{Se}$, and (b) ZnS , $\text{Zn}_{0.75}\text{Cr}_{0.25}\text{S}$ materials.

theoretical nor experimental, were found for comparison. So our work will be a supporting reference for future experimentalists.

The Grüneisen parameter γ is an important thermodynamic quantity, usually used to describe anharmonic effects in the vibrating lattice [42]. It is of considerable interest for both experimental and theoretical investigations. In order to predict the effect of high pressure on the Grüneisen parameter γ of our materials of interest, we have employed the Dugdale and MacDonald model [43]. In this approach, the Grüneisen parameter γ_{D-M} was estimated as follows [43]

$$\gamma_{D-M} = \left(\frac{1}{2}B' + \frac{2}{9} \left(\frac{p}{B} \right) - 1 \right) / \left(1 - \frac{2p}{3B} \right), \quad (10)$$

where B is the bulk modulus, p is the pressure, and B' is the 1st order pressure derivative of the bulk modulus evaluated at different values of pressure p .

Figure 6 discerns the variation of the Grüneisen parameter γ_{D-M} as a function of the pressure p for CdSe , $\text{Cd}_{0.75}\text{Cr}_{0.25}\text{Se}$, ZnS , and $\text{Zn}_{0.75}\text{Cr}_{0.25}\text{S}$ materials. Monotonic and non-linear behavior of γ_{D-M} has been shown under compression for all materials of interest. The results are consistent with the values reported for iridium phosphide (Ir_2P) material [42] using the quasi-harmonic Debye model.

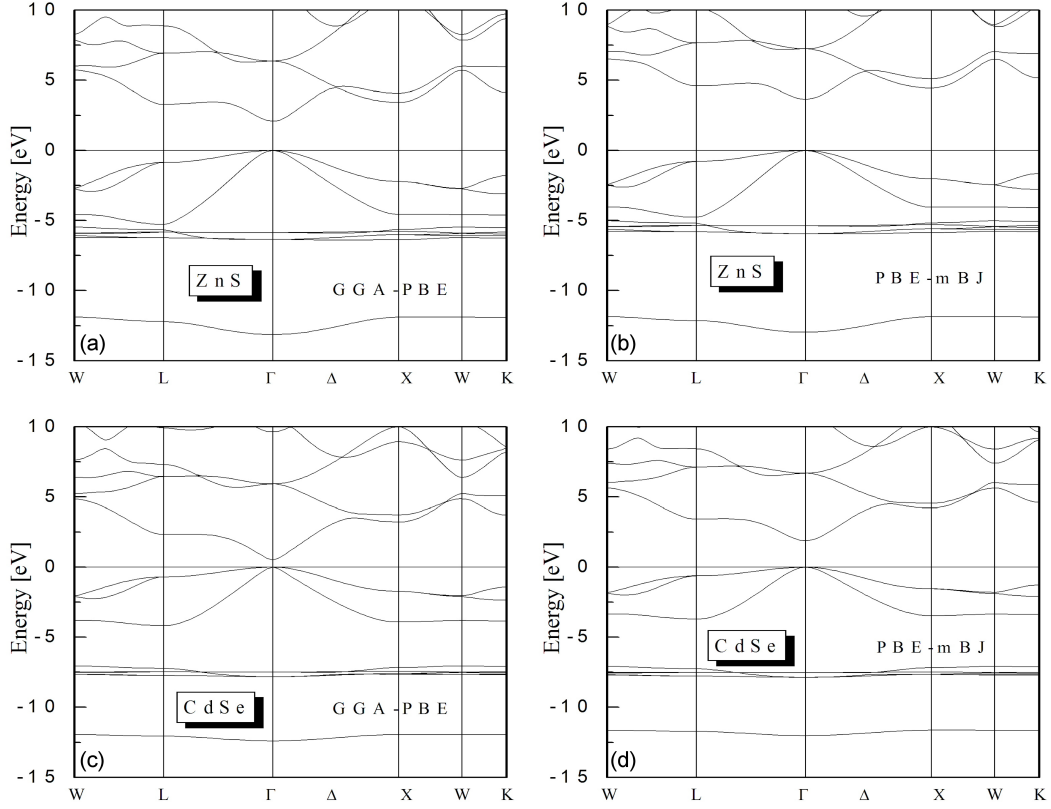


Fig. 7. Band structures of binary compounds CdSe and ZnS using the GGA-PBE and mBJ-GGA-PBE approaches, along the high-symmetry k -path (W–L– Γ –X–W–K).

As the pressure varies from 0 to 2.87 GPa, γ_{D-M} values change from 1.03 to 0.91 for CdSe, and from 1.67 to 1.48 for $\text{Cd}_{0.75}\text{Cr}_{0.25}\text{Se}$, respectively. Meanwhile, the increasing of the pressure from 0 to 14.7 GPa leads to a decrease in the values of γ_{D-M} from 1.21 to 0.88 for ZnS and from 1.29 to 0.93 for $\text{Zn}_{0.75}\text{Cr}_{0.25}\text{S}$, respectively. The zero-pressure value (1.21) of γ_{D-M} obtained here for ZnS is in good agreement with the values (1.17–1.39) reported for the long-wave LA [100] mode Grüneisen parameter γ_{LA} [44]. It is also in excellent agreement with the values (1.08–1.27) reported for LA [110] γ_{LA} [44]. The mode Grüneisen parameters are usually calculated using knowledge of the dependence of phonon frequencies on the volume of the crystal.

It was perceived from the Fig. 6 that the incorporation of 25% Cr atoms into CdSe and ZnS crystals increases the Grüneisen parameter γ_{D-M} for both $\text{Cd}_{0.75}\text{Cr}_{0.25}\text{Se}$ and $\text{Zn}_{0.75}\text{Cr}_{0.25}\text{S}$ alloys. The dispersion on γ_{D-M} values between doped and undoped states is larger for CdSe compound than ZnS. The best fits of γ_{D-M} (is dimensionless) vs pressure p [GPa] obey the following 2nd order polynomial expressions: $\gamma_{D-M} = 1.03 - 0.05p + 2.99 \times 10^{-3}p^2$ for CdSe, $\gamma_{D-M} = 1.66 - 0.08p + 5.62 \times 10^{-3}p^2$ for $\text{Cd}_{0.75}\text{Cr}_{0.25}\text{Se}$, $\gamma_{D-M} = 1.21 - 0.035p + 0.87 \times 10^{-3}p^2$ for ZnS, $\gamma_{D-M} = 1.28 - 0.037p + 0.92 \times 10^{-3}p^2$ for $\text{Zn}_{0.75}\text{Cr}_{0.25}\text{S}$, respectively.

3.2. Electronic band structure and density of states

Knowledge of the energy band structures in semi-conductors provides valuable information regarding their potential use in fabricating electronic devices. In this part of the present contribution, we have focused on the discussion on the electronic properties of ZnS, CdSe, $\text{Cd}_{0.75}\text{Cr}_{0.25}\text{Se}$, and $\text{Zn}_{0.75}\text{Cr}_{0.25}\text{S}$ alloys. Figure 7 displays the comparison of the two methods of calculation for the energy band structure of ZnS and CdSe semi-conductors along the high-symmetry (W–L– Γ –X–W–K) directions in the Brillouin zone. As shown in Fig. 7, the direct band gap energy of ZnS and CdSe of about 2.08 eV and 0.51 eV within GGA-PBE are smaller than that within mBJ-GGA-PBE 3.65 eV and 1.88 eV, which are close to the experimental value of ZnS (3.87 eV) and CdSe (1.84 eV) [45].

The underestimation of the band gap by GGA-PBE is due to the lack of discontinuity in this exchange-correlation potential. Nonetheless, the band gap in GGA-PBE is always smaller than the experimental value. For that case, the researcher developed a few techniques that reduce the usual underestimation problem, including the modified Becke–Johnson approach and Perdew–Burke–Ernzerhof generalized gradient approximation (mBJ-GGA-PBE). However, for $\text{Cd}_{0.75}\text{Cr}_{0.25}\text{Se}$ and $\text{Zn}_{0.75}\text{Cr}_{0.25}\text{S}$ alloys, we focus

TABLE II

Direct band gaps E_g [eV] and total and local magnetic moments [μ_B] within the muffin-tin spheres and in the interstitial sites for $\text{Cd}_{0.75}\text{Cr}_{0.25}\text{Se}$ and $\text{Zn}_{0.75}\text{Cr}_{0.25}\text{S}$ alloys, calculated using the mBJ-GGA-PBE.

Materials	Method	E_g	μ_{tot}	Cr	Cd/Zn	Se/S
$\text{Cd}_{0.75}\text{Cr}_{0.25}\text{Se}$	mBJ-GGA	2.67	4.000	3.628	0.142	-0.05
$\text{Zn}_{0.75}\text{Cr}_{0.25}\text{S}$	mBJ-GGA	3.75	4.000	3.337	0.123	0.01
	Ref. [7]	3.02	4.000	3.329	0.034	-0.006

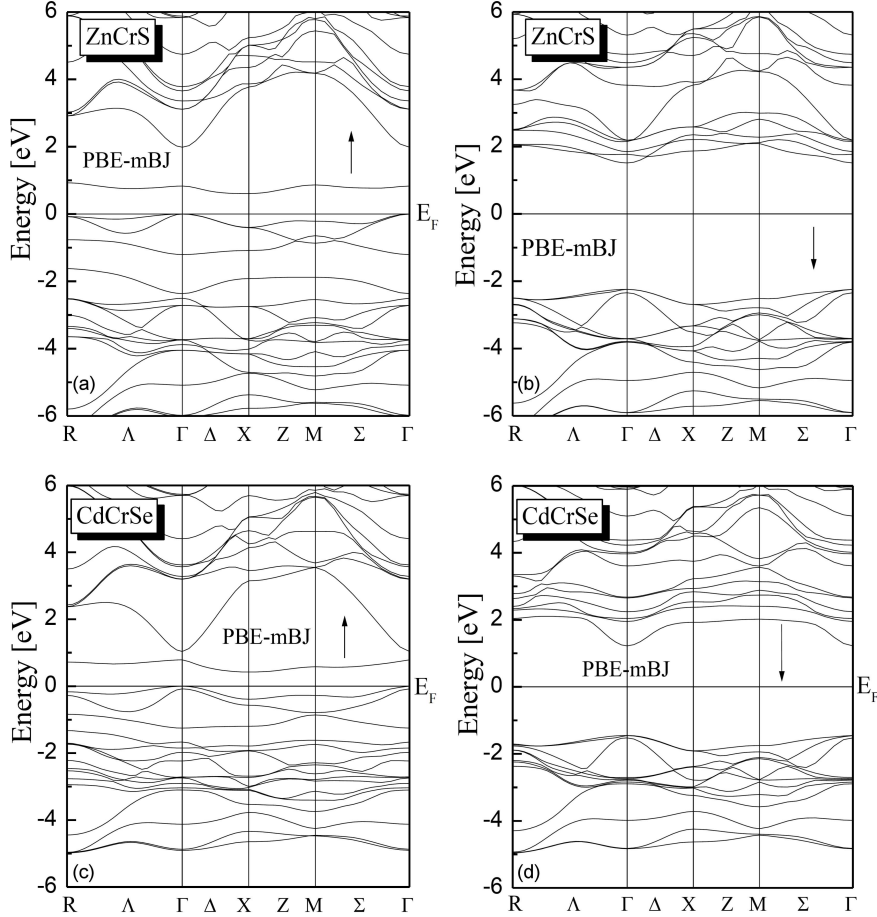


Fig. 8. Spin-polarized band structures for $\text{Cd}_{0.75}\text{Cr}_{0.25}\text{Se}$ and $\text{Zn}_{0.75}\text{Cr}_{0.25}\text{S}$ majority spin and minority spin using the mBJ-GGA-PBE approximation, along the high-symmetry k -path (R- Γ -X-M- Γ).

on the evaluation of band structure and density of states (DOS) that are not influenced by the GGA-PBE approach. The electronic band structures of Cr-doped ZnS and CdSe along high-symmetry points in the first Brillouin zone, calculated using the mBJ-PBE-GGA approaches are displayed in Fig 8. Band structure plotting is done along a specific path, i.e., R to Γ , Γ to X, X to M, and M to Γ , because the case of $x = 0.25$ is obtained by replacing the Cd or Zn atoms at vertex site without changing the other 3Cd or 3Zn atoms, or the 4S (Se) ones. In this way we obtain a cubic structure with space group $P-43m$ (no. 215). The overall band profile shows the same characteristic features for the studied compounds. It is obvious that for all

the cases, there is a large exchange spin-splitting between the majority spin (spin-up) and the minority spin (spin-down) states around the Fermi level, which implies that the addition of a Cr atom can order magnetism in ZnS and CdSe hosts. We see that mBJ-GGA-PBE predicts the ground state to be semiconducting.

The calculated energy band gap $E_g^{\Gamma-\Gamma}$ values for spin-down structures are listed in Table II, along with the predicted data reported by Nazir et al. [7]. The calculated electronic band structure of $\text{Zn}_{0.75}\text{Cr}_{0.25}\text{S}$ material aligns with the results of Nazir et al. [7]. One can see that by applying this method, we do not observe the overlapping of orbitals with the E_F level situated at 0 eV in the

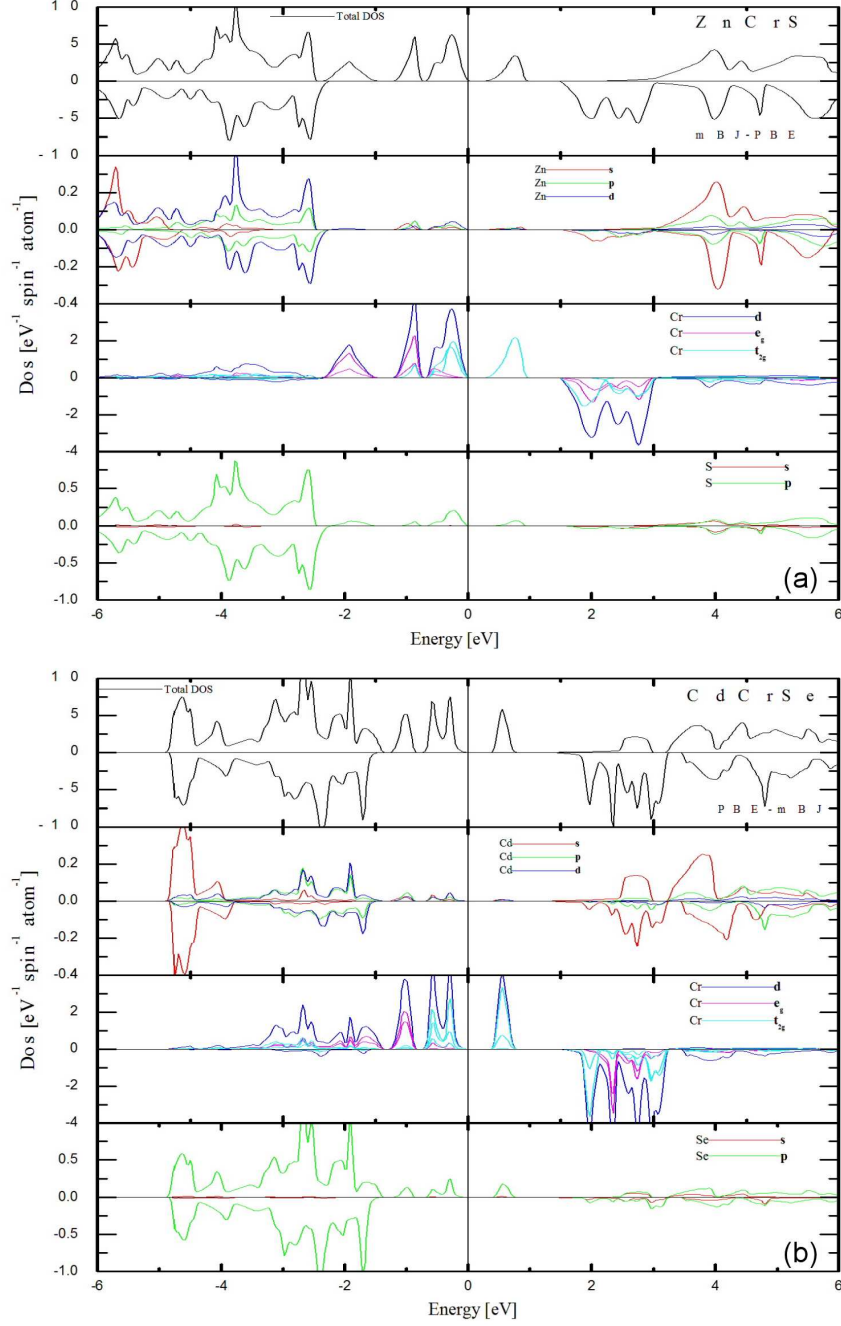


Fig. 9. Spin-dependent total and partial density of states for $\text{Cd}_{0.75}\text{Cr}_{0.25}\text{Se}$, and $\text{Zn}_{0.75}\text{Cr}_{0.25}\text{S}$ alloys using the mBJ-GGA-PBE approximations.

majority spin as observed when we use the purely GGA-PBE and Cr-doped ZnS and CdSe are semiconducting. In Fig. 8, the band structures calculated for $\text{Zn}_{0.75}\text{Cr}_{0.25}\text{S}$ and $\text{Cd}_{0.75}\text{Cr}_{0.25}\text{Se}$ using mBJ-GGA-PBE have an indirect gap $E_g^{X-\Gamma} = 0.60$ eV and 0.42 eV, respectively, in the spin-up channel and direct gap $E_g^{\Gamma-\Gamma} = 3.75$ eV and 2.67 eV, respectively, in the case of the spin-down channel. The value of the band gap in the spin-down state is modified, explaining its behavior toward semiconductors, and hence, it is clear that these materials exhibit spin polarization.

To have a deep insight into band structure, the partial and total densities of states are analyzed, and their spectra are displayed in Fig. 9 with mBJ-GGA-PBE approximation within the energy range of -6 eV to 6 eV. Usually, in the DOS plots, the Fermi energy is placed at zero level [46]. The region located below the Fermi level is the valence band (VB), while that above the empty region devoid of states (DOS-band gap) represents the conduction band (CB) [47]. The overall DOS of the Cr-doped ZnS and CdSe reveal similar contributions in the whole energy range. The observed results of

the alloyed indicate that both compounds present a semiconducting state with a gap for both the majority and minority spins directions. The dopant atom contributed to the Fermi level by the contribution of S/Se- p states. The real cause of the appearance of ferromagnetism has been investigated through the calculated partial density of states (PDOS), as presented in Fig. 9, and it has been found that ferromagnetism arises due to hybridization between Cr $3d$ -states and anion S/Se- p states. Moreover, the Cr- d orbitals split into e_g and t_{2g} orbitals, as shown in Fig. 9. Both e_g and t_{2g} orbitals are only partially filled, i.e., only the majority spin bands of Cr^{2+} ions are occupied, whereas all the minority spin bands of Cr^{2+} ions are empty. Above the gap, we observe the lowest group of conduction bands, the bottom of which is derived mostly from Cd (Zn) s states for spin-up and an admixture of Cd(Zn) s states and Cr d states for spin-down. Figure 9 shows also that there is a strong hybridization between the $3d$ -Cr and the anion (S/Se) p . The separation between the spin-up and spin-down peaks is known as spin-exchange splitting, which is represented by $(\Delta x(d) = d \downarrow - d \uparrow)$, and its values for Cr $3d$ states of $\text{Cd}_{0.75}\text{Cr}_{0.25}\text{Se}$ and $\text{Zn}_{0.75}\text{Cr}_{0.25}\text{S}$ are found, using mBJ-GGA-PBE, to be 3.22 eV and 3.17 eV, respectively. We will see clearly what the differences mean, by the introduction of mBJ-GGA-PBE and its influence on the obtained results, especially on the band structures and density of states. It is particularly helpful in understanding more precisely the bands whose electrons are strongly correlated.

3.3. Magnetic properties

In order to give more information on the magnetic properties of $\text{Cd}_{0.75}\text{Cr}_{0.25}\text{Se}$ and $\text{Zn}_{0.75}\text{Cr}_{0.25}\text{S}$ materials, we calculate the total and local magnetic moments. The obtained values for both alloys using the mBJ-GGA-PBE approximation are also reported in Table II. The total magnetic moment per formula unit μ_{tot} of $\text{Cd}_{0.75}\text{Cr}_{0.25}\text{Se}$ is $4.00 \mu_B$, while that of $\text{Zn}_{0.75}\text{Cr}_{0.25}\text{S}$ is found to be $4.00 \mu_B$. This later value ($4.00 \mu_B$) agrees well with another theoretical result ($4 \mu_B$) by Nazir et al. [7]. The near integer value of the total magnetization is consistent with the half-metallic characteristic of these materials. Furthermore, the μ_{tot} of $\text{Cd}_{0.75}\text{Cr}_{0.25}\text{Se}$ and $\text{Zn}_{0.75}\text{Cr}_{0.25}\text{S}$ calculated here are almost equal to the value ($4 \mu_B$) reported for both RbMnSe_2 and CsMnSe_2 [48].

The main source of magnetization in these two materials is the unfilled Cr- $3d$ states. The origin of the Cr magnetic moment can be related to the partially filled t_{2g} level in the $3d$ state [49]. The change in the net magnetic moment of a material is because of the negative p - d coupling between Cr- $3d$ and Se(S)- p states (in Cr-doped semiconductors). This negative coupling lowers the total energy, which stabilizes the magnetic configuration of the compounds.

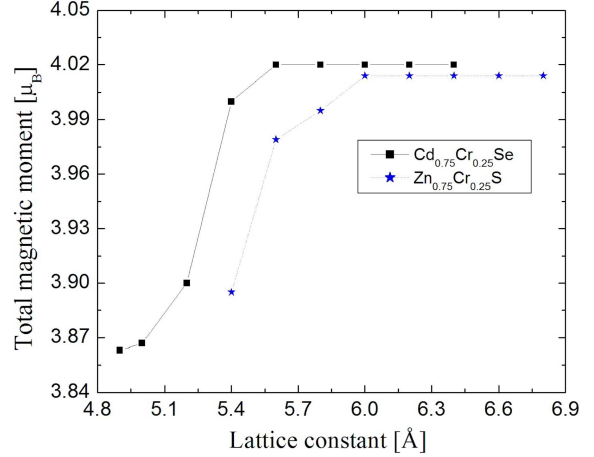


Fig. 10. Total magnetic moment μ_{tot} vs the lattice constant for both $\text{Cd}_{0.75}\text{Cr}_{0.25}\text{Se}$ and $\text{Zn}_{0.75}\text{Cr}_{0.25}\text{S}$ alloys.

TABLE III

Spin-exchange splitting energy $\Delta_x d$, $\Delta_x(pd)$ and exchange constants $N_{0\alpha}$ and $N_{0\beta}$ for $\text{Cd}_{0.75}\text{Cr}_{0.25}\text{Se}$ and $\text{Zn}_{0.75}\text{Cr}_{0.25}\text{S}$ alloys, calculated using the mBJ-GGA-PBE approximation.

Materials	Method	$\Delta_x d$	$\Delta_x(pd)$	$N_{0\alpha}$	$N_{0\beta}$
$\text{Cd}_{0.75}\text{Cr}_{0.25}\text{Se}$	mBJ-GGA	3.22	-1.44	1.80	-2.88
$\text{Zn}_{0.75}\text{Cr}_{0.25}\text{S}$	mBJ-GGA	3.17	3.17	1.36	-4.48
	Ref. [7]	-	-	0.24	-5.02

The exchange constants $N_{0\alpha}$ and $N_{0\beta}$ show the contribution of the valence and conduction bands (VB and CB) in the process of exchange and splitting and can be related to the spin-splitting at the gamma symmetry point of a band structure. These parameters ($N_{0\alpha}$ and $N_{0\beta}$) are calculated directly from the conduction band-edge spin-splitting ($\Delta E_c = E_c(\downarrow) - E_c(\uparrow)$) and valence band-edge spin-splitting ($\Delta E_v = E_v(\downarrow) - E_v(\uparrow)$) for both $\text{Cd}_{0.75}\text{Cr}_{0.25}\text{Se}$ and $\text{Zn}_{0.75}\text{Cr}_{0.25}\text{S}$ materials. Assuming the usual Kondo interaction, $N_{0\alpha}$ and $N_{0\beta}$ are defined [50–52] as

$$N_{0\alpha} = \frac{\Delta E_c}{x \langle s \rangle}, \quad N_{0\beta} = \frac{\Delta E_v}{x \langle s \rangle}, \quad (11)$$

where $\langle s \rangle$ is one half of the calculated magnetization per Cr ion, while x denotes the doping concentration.

Our values of the spin-exchange splitting energy $\Delta_x d$ and $\Delta_x(pd)$, and exchange constants ($N_{0\alpha}$ and $N_{0\beta}$) for ferromagnetic $\text{Cd}_{0.75}\text{Cr}_{0.25}\text{Se}$ and $\text{Zn}_{0.75}\text{Cr}_{0.25}\text{S}$, calculated using mBJ-GGA-PBE are listed in Table III, along the theoretical values [7].

We have also calculated, using mBJ-GGA-PBE, the exchange splitting energy ($\Delta x(d) = d \downarrow - d \uparrow$), which is defined as the separation between the spin-up and spin-down peaks, to explore the

existence of a stable ferromagnetic state. In order to illustrate and quantify the nature of the attraction in these DMSs, we calculate the exchange splitting ($\Delta x(pd) = Ev \downarrow - Ev \uparrow$) of the valence bands top for the spin up and down orientations. The negative exchange-splitting gap $\Delta x(pd)$ values mean that the effective potential for the minority spin is more attractive as compared to the majority spin, which characterizes the spin-polarized systems. We can also deduce from these results that mBJ-GGA-PBE influences the positions of the electronic states and that the $N_{0\alpha}$ constant are positive for both compounds. The direct relation between the exchange constant and band gap confirms the ferromagnetic nature of these materials [7].

Finally, we present in Fig. 10 the μ_{tot} of both $\text{Cd}_{0.75}\text{Cr}_{0.25}\text{Se}$ and $\text{Zn}_{0.75}\text{Cr}_{0.25}\text{S}$ alloys as a function of the lattice constant. It is observed that μ_{tot} remains unchanged with the change of lattice parameters until the lattice constants are compressed to the critical values of 6.0 Å and 5.4 Å for $\text{Cd}_{0.75}\text{Cr}_{0.25}\text{Se}$ alloy and $\text{Zn}_{0.75}\text{Cr}_{0.25}\text{S}$ material, respectively. Similar behavior of the total magnetic moment versus the lattice parameter was also observed for both $\text{Zn}_{0.75}\text{Cr}_{0.25}\text{Te}$ and $\text{Cd}_{0.75}\text{Cr}_{0.25}\text{Te}$ ternary alloys [51].

4. Conclusion

In summary, we studied in detail the structural, thermodynamic, electronic, and magnetic properties of $\text{Cd}_{1-x}\text{Cr}_x\text{Se}$ and $\text{Zn}_{1-x}\text{Cr}_x\text{S}$ with $x = 0.25$ by performing the first-principles calculations within the GGA-PBE and mBJ-GGA-PBE approximations for the exchange-correlation functional. The parameters of the structure, as well as the effect of high pressures on the relative volume variation, the isothermal bulk modulus B , and the Grüneisen parameter for CdSe and ZnS binary compounds as well as for $\text{Cd}_{0.75}\text{Cr}_{0.25}\text{Se}$ and $\text{Zn}_{0.75}\text{Cr}_{0.25}\text{S}$ ternary alloys, were predicted and discussed. We found that $\text{Cd}_{0.75}\text{Cr}_{0.25}\text{Se}$ material is more compressible than $\text{Zn}_{0.75}\text{Cr}_{0.25}\text{S}$ alloy. The quasi-harmonic Debye model is successfully applied to determine some of the thermodynamic properties, such as entropy and heat capacity. The analysis of the electronic and magnetic properties shows that both $\text{Cd}_{0.75}\text{Cr}_{0.25}\text{Se}$ and $\text{Zn}_{0.75}\text{Cr}_{0.25}\text{S}$ ternary alloys are ferromagnetic semiconductors, as observed using the mBJ-GGA-PBE approach. The ferromagnetic behavior is verified by the asymmetric density of states in both spin channels and the optimized energy volume curve in the spin-polarized calculation. The total magnetic moments of $\text{Cd}_{0.75}\text{Cr}_{0.25}\text{Se}$ and $\text{Zn}_{0.75}\text{Cr}_{0.25}\text{S}$ mainly arise from the Cr atom with a small contribution from the Se(S) and Cd(Zn) atoms. Furthermore, the results of the exchange splitting produced by the Cr d states $\Delta_x d$ and $\Delta_x(pd)$ show that the effective potential for the minority spin is more attractive than that of the majority spin.

References

- [1] J.K. Furdyna, *J. Appl. Phys.* **53**, 7637 (1982).
- [2] J. K. Furdyna, *J. Appl. Phys.* **64**, R29 (1988).
- [3] J.K. Furdyna, J. Kossut, *Diluted Magnetic Semiconductors*, Vol. 25, Academic, New York 1988.
- [4] C.M. Fang, G.A. Wijs, R.A. Groot, *J. Appl. Phys.* **91**, 8340 (2002).
- [5] R.A. Stern, T.M. Schuler, J.M. MacLaren, D.L. Ederer, *J. Appl. Phys.* **95**, 7468 (2004).
- [6] Y. Saeed, S. Nazir, A. Shaukat, A.H. Reshak, *J. Magn. Magn. Mater.* **322**, 3214 (2010).
- [7] S. Nazir, N. Ikram, S. Siddiqi, Y. Saeed, A. Shaukat, A.H. Reshak, *Curr. Opin. Solid State Mater. Sci.* **14**, 1 (2010).
- [8] S. Amari, S. Méçabih, B. Abbar, B. Bouhaf, *J. Magn. Magn. Mater.* **324**, 2800 (2012).
- [9] C. Bourouis, A. Meddour, *J. Magn. Magn. Mater.* **324**, 1040 (2012).
- [10] H. Saito, V. Zayets, S. Yamagata, K. Ando, *Phys. Rev. B* **66**, 081201 (2002).
- [11] W. Mac, A. Twardowski, P. Eggenkamp, H. Swagten, Y. Shapira, M. Demianiuk, *Phys. Rev. B* **50**, 14144 (1994).
- [12] W. Mac, N.T. Khoi, A. Twardowski, M. Demianiuk, *J. Cryst. Growth.* **159**, 993 (1996).
- [13] M. Herbich, W. Mac, A. Twardowski, K. Ando, D. Scalbert, A. Petrou, M. Demianiuk, *J. Cryst. Growth.* **184–185**, 1000 (1998).
- [14] P. Blaha, K. Schwarz, G.K.H. Madsen, D. Kvanicka, J. Luitz, “WIEN2K, An Augmented Plane Wave + Local Orbital Program for Calculating Crystal Properties”, Techn. Universitat Wien, Wien 2001.
- [15] J.P. Perdew, K. Burke, M. Ernzerhof, *Phys. Rev. Lett.* **77**, 3865 (1996).
- [16] F. Tran, P. Blaha, *Phys. Rev. Lett.* **102**, 226401 (2009).
- [17] *Landolt-Börnstein Numerical Data and Functional Relationships in Science and Technology, New Series, Group III: Crystal and Solid State Physics, Vol. 22: Semiconductors*, Ed. O. Madelung, Springer-Verlag, Berlin 1987.
- [18] M.A. Blanco, E. Francisco, V. Luaña, *Comput. Phys. Commun.* **158**, 57 (2004).
- [19] B. Ghebouli, M.A. Ghebouli, M. Fatmi, A. Bouhemadou, *Solid State Commun.* **150**, 1896 (2010).

- [20] T. Yang, X. Zhu, J. Ji, J. Wang, *Sci. Rep.* **10**, 3265 (2020).
- [21] I. Asfour, H. Rached, D. Rached, M. Caid, M. Labair, *J. Alloy. Compd.* **742**, 736 (2018).
- [22] S. Amari, R. Mebsout, S. Mécabih, B. Abbar, B. Bouhafs, *Intermetallics* **44**, 26 (2014).
- [23] F.D. Murnaghan, *Proc. Natl. Acad. Sci. USA* **30**, 5390 (1944).
- [24] S. Nazir, N. Ikram, M. Tanveer, A. Shaukat, Y. Saeed, A.H. Reshak, *J. Phys. Chem. A* **113**, 6022 (2009).
- [25] S. Mécabih, K. Benguerine, N. Bensoman, B. Abbar, B. Bouhafs, *Physica B* **403**, 3452 (2008).
- [26] S. Wei, A. Zunger, *Phys. Rev. B* **35**, 2340 (1987).
- [27] S. Narain, *Phys. Status Solidi B* **182**, 273 (1994).
- [28] H. Rekab-Djabri, S. Daoud, M.M. Abdus Salam, S. Louhibi-Fasla, *Acta Phys. Pol. A* **140**, 34 (2021).
- [29] S.A. Al'fer, V.F. Skums, *Inorg. Mater.* **37**, 1237 (2001).
- [30] S. Adachi, *Properties of Group-IV, III-V and II-VI Semiconductors*, John Wiley & Sons, 2005.
- [31] P. Vinet, J.H. Rose, J. Ferrante, J.R. Smith, *J. Phys. Condens. Matter.* **1**, 1941 (1989).
- [32] F. Okba, R. Mezouar, *J. Nano-Electron. Phys.* **14**, 04004 (2022).
- [33] S. Daoud, N. Bioud, P.K. Saini, *J. Magnes. Alloys.* **7**, 335 (2019).
- [34] S. Daoud, N. Bouarissa, A. Benmakhlouf, O. Allaoui, *Phys. Status Solidi B* **257**, 1900537 (2020).
- [35] D. Zhou, T. Su, H. Song, C. Lu, Z. Zhong, Z. Lu, C. Pu, *J. Alloys Compd.* **648**, 67 (2015).
- [36] M. Zhong, H. Qin, Q.-J. Liu, F.-S. Liu, B. Tang, *Phys. Status Solidi B* **256**, 1800440 (2019).
- [37] S. Daoud, N. Bouarissa, H. Rekab-Djabri, P.K. Saini, *Silicon* **14**, 6299 (2022).
- [38] R. Masrour, A. Jabar, S. Labidi, Y. El Krimi, M. Ellouze, M. Labidi, A. Amara, *Mater. Today Commun.* **26**, 101772 (2021).
- [39] E.B. Elkenany, A.R. Degheidy, O.A. Alfrwani, *Silicon* **11**, 919 (2019).
- [40] A.T. Petit, P.L. Dulong, *Ann. Chim. Phys.* **10**, 395 (1819).
- [41] S. Amari, S. Daoud, *Comput. Condens. Matter.* **33**, e00764 (2022).
- [42] Z.J. Liu, T. Song, X-W. Sun, Q. Ma, T. Wang, Y. Guo, *Solid State Commun.* **253**, 19 (2017).
- [43] J.S. Dugdale, D.K.C. MacDonald, *Phys. Rev.* **98**, 1751 (1955).
- [44] T. Soma, H. Matsuo Kagaya, *Phys. Status Solidi B* **135**, K103 (1986).
- [45] W.A. Harrison, *Elementary Electronic Structure*, World Scientific, 1999.
- [46] H. Rekab-Djabri, S. Louhibi-Fasla, S. Amari, S. Bahlouli, M. Elchikh, *Eur. Phys. J. Plus* **132**, 471 (2017).
- [47] N. Sharma, D. Chandra, A. Rathi, A.K. Singh, *Mater. Sci. Semicond. Process.* **151**, 107033 (2022).
- [48] A. Benmakhlouf, A. Bentabet, A. Bouhemadou, A. Benghia, *J. Magn. Magn. Mater.* **399**, 179 (2016).
- [49] S.Y. Wu, H.X. Liu, L. Gu, R.K. Singh, L. Budd, M. van Schilfgaarde, M.R. McCartney, D.J. Smith, N. Newman, *Appl. Phys. Lett.* **82**, 3047 (2003).
- [50] J.A. Gaj, R. Planel, G. Fishman, *Solid State Commun.* **29**, 435 (1979).
- [51] S. Amari, S. Mécabih, B. Abbar, B. Bouhafs, *Comput. Mater. Sci.* **50**, 2785 (2011).
- [52] M. Sajjad, S.M. Alay-e-Abbas, H.X. Zhang, N.A. Noor, Y. Saeed, I. Shakir, A. Shauka, *J. Magn. Magn. Mater.* **390**, 78 (2015).